Multicriteria Sensitivity Analysis for Numerical Model Validation of Experimental Data

Indriyantho, Bobby Rio; Purnomo, Joko; Purwanto; Ottele, Marc; Han, Ay Lie; Gan, Buntara Sthenly

DOI
10.14716/ijtech.v15i6.7146

Publication date
2024

Document Version
Final published version

Published in
International Journal of Technology

International Journal of Technology 15(6) 1644-1662 (2024)
Received June 2024/ Revised October 2024 / Accepted November 2024

International Journal of Technology

http://ijtech.eng.ui.ac.id

Multicriteria Sensitivity Analysis for Numerical Model Validation of Experimental Data

Bobby Rio Indriyantho[1*], Joko Purnomo[2], Purwanto[1], Marc Ottele[3], Ay Lie Han[1], Buntara Sthenly Gan[4]

[1]*Department of Civil Engineering, Universitas Diponegoro, Semarang, 50275, Indonesia*
[2]*Department of Civil Engineering, Petra Christian University, Surabaya, 60236, Indonesia*
[3]*Department of Materials, Mechanics, Management & Design, Delft University of Technology, 2628 CN Delft, The Netherlands*
[4]*Department of Architecture, College of Engineering, Nihon University, Koriyama, 963-8642, Japan*

Abstract. Sensitivity analysis is a decisive step in experimental and numerical structural mechanics. The analysis of structural model quantifies the importance of each input parameter, potential interaction and effects on structural response. Therefore, this study aimed to help reduce the uncertainty surrounding major variables, providing valuable guidance for conducting future experiments. During the investigation, numerically deterministic sensitivity analysis based on multicriteria model evaluations of load-displacement curves representing actual behavior of the member correctly, were reviewed. Multicriteria model combined the evaluation of peak load, energy dissipation before ultimate loading, and toughness of load-displacement response. The methodology led to a strong sensitivity analysis method, generating an agreement between numerical and experimental responses. Moreover, an investigation of the method was presented for a geopolymer haunch, the numerical model was based on rigid body spring model (RBSM), which enabled precise behavior simulation of reinforced concrete structures. RBSM was refined, enabling in-depth evaluation of stress-strain contours, plasticity index, initial crack formation and crack propagation, as well as RBSM-spring failure modes. The proposed multicriteria sensitivity analysis can be implemented with other simulation methods, such as finite element analysis (FEA) and structural simulation software. The recommended method is applicable to any structural member, where laboratory-tested full-scale specimens were functioning as validation tools. Following the proposed multicriteria sensitivity analysis, experimental load-displacement curves of this study supported the results of numerical RBSM in an acceptable range of error predictions.

Keywords: Deterministic sensitivity analysis; Experimental validation; Multicriteria model analysis; Rigid body spring model

1. Introduction

A numerical model is a method that provides detailed visualizations of how composite elements behave under stress-strain contours, individual evolution, initial cracking and crack propagations, as well as the plasticity index. However, this information complicates the precision instruments and laboratory equipment, which cannot be captured by experimental testing. A validation process for full-scale identical laboratory-tested

*Corresponding author's email: bobbyrio@live.undip.ac.id; Tel.: +6224-7474770; Fax: +6224-7460060
doi: 10.14716/ijtech.v15i6.7146

specimens should be conducted to evaluate and further improve numerical models until the predetermined level of correctness is achieved.

Numerical models assume ideal conditions, including perfect material properties, precise member dimensions and loading conditions, which differs from real-world tested members that inevitably have imperfections. The incompatibilities between model and experimental data lead to deviations including actual and numerically obtained load-displacement curves.

Previously, finite element method (FEM) was used to simulate load-displacement behavior and failure mode of a geopolymer haunch beam-to-column connection (Purwanto *et al.,* 2023; Purwanto, 2021). This model failed to simulate the concrete fracture in the compression zone correctly. FEM over-estimated the ultimate load response, initial stiffness before reinforcement yielding and strain energy dissipation even with extensive sensitivity analysis adjustments. A major factor was the assumption of a perfect bond between geopolymer haunch, beam-column element, and all steel reinforcements. Although the shear behavior between geopolymer and conventional concrete was studied (Purwanto *et al.,* 2022), the data were not implemented into model. Other factors included imperfection of the members, irregular thicknesses throughout the length of the beam, non-homogeneous material properties, and vibration disturbances during loading, among others. Compared to FEM, the rigid body spring model (RBSM) provides a better representation for complex cases including multiple elements and materials. RBSM has been used to simulate the behavior of concrete flexural elements externally reinforced with carbon fiber reinforced polymers (CFRP) with satisfactory results (Purnomo *et al*., 2023a; 2023b). However, the predicted curves still showed significant deviation from the actual behavior.

The behavior of geopolymer elements has been numerically investigated extensively in the past years, and the flexure response of geopolymer beam-elements using finite element analyses (FEA) was studied by many investigations (Aziz *et al.,* 2022; Darmawan *et al.,* 2022; Hassan *et al.,* 2022; Chong *et al.,* 2022; Venkatachalam *et al.,* 2021). Following this discussion, the majority modeled the load-displacement and stress-strain response of a range of simply-supported members subjected to four- or three-point loading systems and compared the behavior to identical conventional concrete members. More recently, RBSM was developed to simulate flexure behavior of FRP-reinforced members (Ahmed *et al*., 2020; Purnomo *et al*., 2023b). FRP-to-concrete debonding mechanism was studied by (Farah and Sato, 2007; Jiang *et al*., 2023) using normal and shear springs in the interface. The failure mode was distinguished by concrete failure and a combination of adhesive and concrete failure. Moreover, special topics on shear phenomenon were modeled using RBSM (Fu *et al.,* 2023; Zheng, Fu, and Wang, 2021), and the response of frost, thaw, and freeze was studied by (Gong *et al.,* 2015). The only fiber-reinforced concrete study was conducted recently, using steel fibers by (Sarraz, Nakamura, and Miura, 2023; Sarraz *et al.,* 2022).

RBSM is of the utmost appropriateness to represent cementitious materials. The model is characterized by its ability to simulate the concrete micro-cracking behavior based on the disparity between high compression and weak tensile strengths. The combination of biaxial compression provides additional strength due to the confinement effect that can be accommodated in model (Jaiswal and Murty, 2024; Wei and Ren, 2023; Ottosen and Ristinmaa, 2005). Additionally, numerical model requires sensitivity analysis to ensure the correctness of model in representing experimental specimen. An overview of concrete FEM including the general sensitivity analyses is presented by (Kagermanov and Markovic, 2023). Artificial intelligence and machine learning recently became favored as sensitivity analysis tool by evaluating the influence of parameters of model (Nafees *et al.*, 2022; Li *et*

al., 2021; Feng and Fu, 2020). Meanwhile, probabilistic sensitivity analysis of concrete-based specimens proved efficient in determining the degree of uncertainty factors (Ferro and Pavanello, 2023; Blagojević *et al*., 2021).

The validation member in this study was a full-scale haunch beam-to-column element constructed of conventional concrete. The haunch was made of self-compacting geopolymer concrete (SCGC) which was mandatory to overcome the small casting space of the haunch (Purwanto *et al*., 2022; Purwanto, 2021; Purwanto and Indarto, 2019). Moreover, the element was subjected to a monotonic loading-unloading, displacement-controlled scheme up to failure (Purwanto *et al.*, 2023). The haunch improved the load-carrying capacity and performance of flexural member. Geopolymer concrete is a green, environmentally friendly waste material requiring zero cement in its production (Petrus *et al*., 2021; Thang, Thach, and Minh, 2021). Experimental testing of this type of specimen is elaborate, costly, and time-consuming. Imperfections and irregularities of specimen create divergences between perfect numerical model and experimental data. Therefore, numerical model does not present the real behavior to a high precision degree. Models that enable accurate representation of experimental load-displacement responses are a valuable tool for analyzing a broad range of variables in the assemblage. The corrected model provides information that cannot be obtained from visual observations of laboratory-based experimental.

Strong deterministic multicriteria sensitivity analysis was introduced to represent the load-displacement behavior of actual, laboratory-tested identical specimens. This newly-developed multicriteria sensitivity method was accessed to adjust numerically-obtained responses to the real-time behavior incorporating irregularities and imperfections. The model analyses included sensitivity examination based on peak load, energy dissipation of load-displacement curve before ultimate loading, and toughness of the member through the analysis of post-peak energy. Following this discussion, the validated model was used to study concrete areas prone to tensile stresses, to identify opportunities for improvement and optimization. This proposed method could be implemented into any nonlinear software program or FEA model.

2. Materials and Methods

2.1. Experimental Works

Flexural beam-to-column specimens with a length of 3.50 m were cast monolithically using conventional concrete with a 28-day cylindrical compressive strength f_c' = 31.11 MPa. The concrete was a self-compacting concrete (SCC), according to (Purwanto *et al.*, 2023; Purwanto, 2021). During this study, targeted compression strength of 30 MPa was designed based on job-mix procedure for both conventional and geopolymer concrete to reduce strain disparities between beam-column and haunch under loading. The primary purpose of this method was to obtain the material mix proportions. During the process, the job mix led to conventional mix proportion as shown in Table 1.

Table 1 Conventional concrete mix design properties by weight

Materials	Composition
aggregate: cement paste	70% : 30%
coarse aggregate: fine aggregate	60% : 40%
cement: water	65% : 35%

28-day cylinder compression strength led to a strength of 31.11 MPa, which was in the margins of the design. During this study, mix of geopolymer concrete was obtained in an

identic manner leading to the proportions as shown in Table 2. Cement paste used in this process was replaced by fly ash and alkaline activator generally known as binder.

Table 2 Geopolymer concrete mix design properties by weight

Materials	Composition
aggregate : binder	70% : 30%
coarse aggregate : fine aggregate	60% : 40%
fly ash : alkaline activator	65% : 35%
Na_2SiO_3 Be-52 : NaOH (12 M)	2.5 : 1.0
extra water	11.70% of binder
extra cement	5.77% of binder
superplasticizer	2.00% of fly ash

The geopolymer concrete used in this study had a strength of 32.52 MPa. The targeted 28-day compressive strength of 30 MPa was exceeded by 8%, which was in the acceptable limits. The substitution of cement paste as a binder in SCGC was a mixture of fly ash class F and alkaline activator, where the activator consisted of sodium hydroxide (NaOH) with molarity of 12 M and sodium metasilicate (Na_2SiO_3) type Be-52. Superplasticizer was added to SCGC mix to produce highly flowable concrete. Meanwhile, adding small amounts of cement and water functioned as a spark to activate the superplasticizer. According to (Purwanto *et al.*, 2023; Purwanto, 2021), the concrete mix was poured through narrow-casting inlets with a 20 mm to 40 mm dimension. SCGC was the best option to obtain good homogeneity without vibration compaction (Ulhaq and Andayani, 2021). The mix design of this type of concrete was studied extensively (Ghafoor and Fujiyama, 2023; Kanagaraj *et al.*, 2023; Kumar and Raguraam, 2018). An elaborate review of this topic was found in the work of (Thakur and Bawa, 2022).

During the process, the specimens were reinforced by four deformed rebars with a diameter of 13 mm at the tensile zone (4D13) and two rebars with the same diameter at the compressive one (2D13). In comparison, the column was reinforced with three rebars on each side of eight in total (8D13). The beam and column had stirrups with a diameter of 8 mm and a 50 mm spacing (Figure 1). Additionally, the reinforcement had a yield strength f_y of 360 MPa, where its ultimate strength f_u was 460 MPa, and the haunch had an angle of 26.5°.

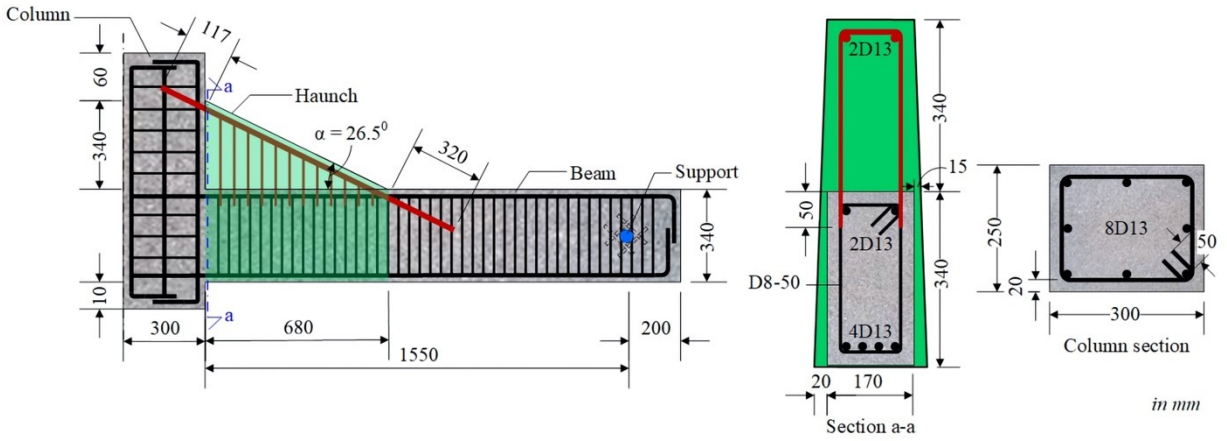

Figure 1 Reinforcement detail of beam-column joint.

The determination of haunch angle was based on the study of influence of angle on effectiveness of the haunch in shifting the formation of plastic joint (Purwanto, 2021). Figure 2a showed the measured strain of tensile reinforcement, while Figure 2b graphically showed the gradient of strain in the beam as a function of haunch length. The study signified

that for the prismatic member, formation of plastic joint occurred at beam-column face. Haunch angle of 14^0 reduced the stain but was unable to relocate plastic joint formation. 26.5^0 angle clearly showed that the largest stain was located at haunch-tip. Following this discussion, an angle of 26.5^0 effectively utilized the haunch.

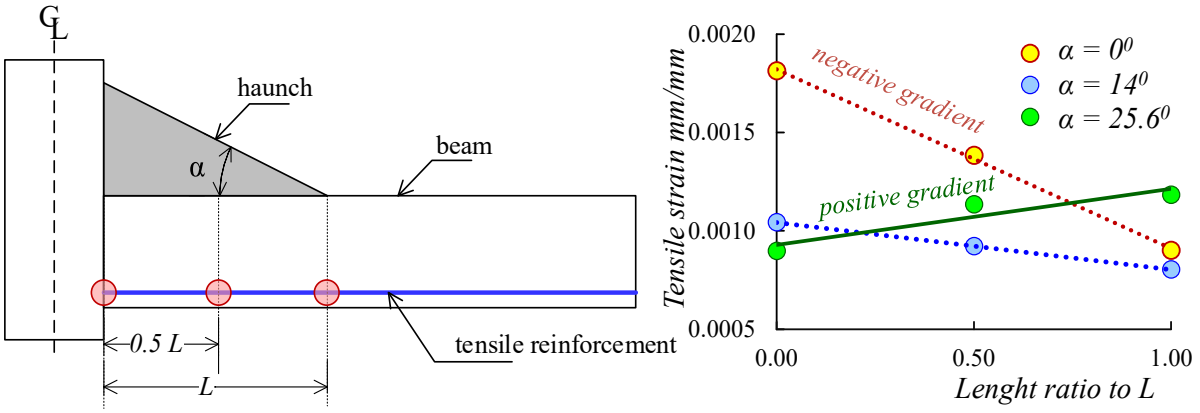

(a) Location of strain measurement relative to the haunch-length

(b) Tensile strain gradient for a 0^0 (prismatic), 14^0 and 26.5^0 haunch angle

Figure 2 Strain in tensile reinforcement as a function of haunch angle.

Reinforcement configuration was based on the principles of an under-reinforced beam, and considering the spacing in between reinforcement to ensure that concrete was well poured and homogeneously compacted. The haunch beam-column specimen was tested monotonically with a loading-unloading scheme. In addition, the load was applied at the center of the column. Displacement-controlled testing was performed until the specimen achieved the ultimate load-carrying capacity. Relating to this process, experimental test setup was shown in Figure 3. To record the load and the displacement, load cells and LVDTs (linear variable differential transformers) were installed and connected to a data logger.

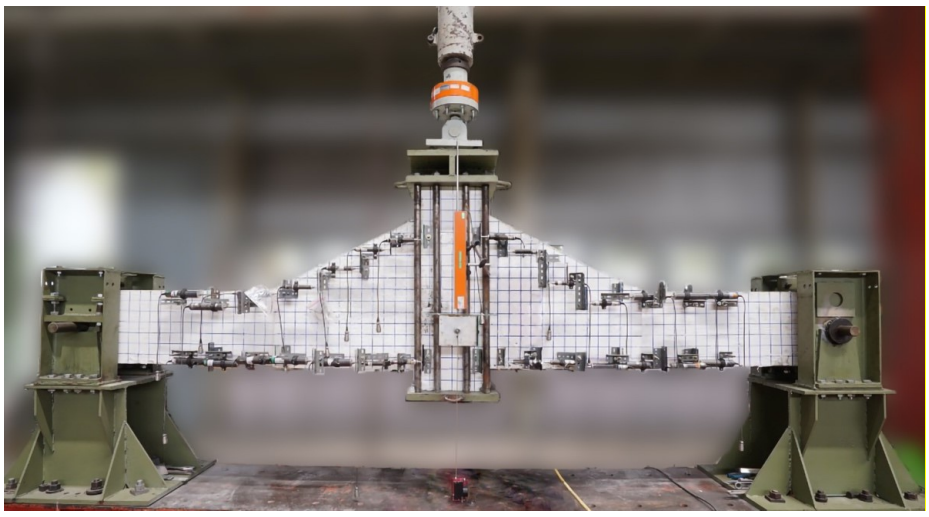

Figure 3 Experimental test setup (Purwanto *et al.*, 2023)

In experimental studies, non-uniformity of material properties, where dimensions of elements that were less accurate and precise, imperfect configuration and position of longitudinal reinforcement and stirrups, casting systems causing non-homogeneity as well as density of concrete were expected to occur. The loading procedure was also very responsive to vehicle action, vibrating the surrounding testing location. All these factors led to a load-displacement response including imperfections.

2.2. RBSM

Model was discretized into a series of rigid body plane stress elements interconnected by normal and shear springs at individual interfaces (Takeuchi, 2005). Orthotropic plane stress elements were used to model the concrete and steel reinforcement. Figure 4 showed the displacement field of isotropic plane stress element for the concrete element.

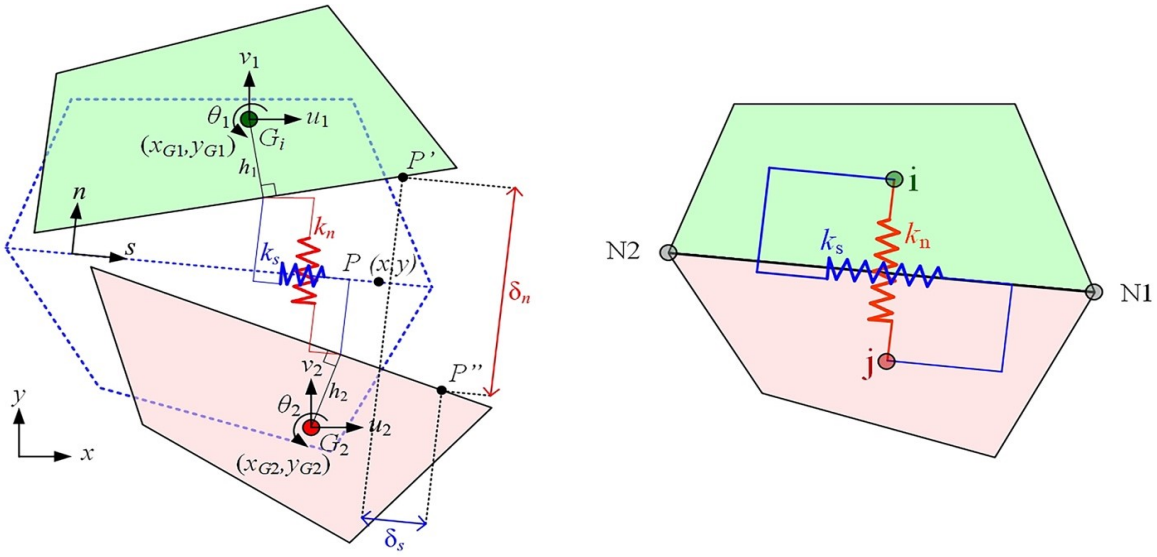

Figure 4 Displacement and kinematics of the isotropic plane stress element

Each element had three degrees of freedom, namely horizontal displacement (u_i), vertical displacement (v_i), and rotational displacement (q_i), respectively. In this study, *xy*-axis and *ns*-axis represented the global and local coordinate systems, respectively. Point *P* was an arbitrary point at the interface between two adjacent elements. After the elements were displaced, this point was separated and attached to adjacent boundaries of the elements represented by *P'* and *P"* in Figure 4. The relative displacement between centroid (G_i) of elements was expressed in the normal (d_n) and tangential (d_s) direction to the interface (Purnomo *et al.*, 2023a). Moreover, stress-strain relationship in the springs was established by reviewing kinematics between the two displaced elements. The determination of spring failure was justified based on Mohr-Coulomb criteria.

Cumulative displacement ($\boldsymbol{\delta}_c$) was evaluated by summing the displacement of each element as described in Equation 1, where $\mathbf{u}_i$ represented the degrees of freedom, and $\mathbf{B}_i$ was defined in Equation 2. In the Equation, l_i and m_i represented the direct cosines, while x_{iG} and y_{iG} signified the centroid of each element. The strain on the springs was calculated based on Equation 3. Stress-strain matrix was expressed by Equation 4, where $\mathbf{D}_c$ represented the concrete material matrix as defined in Equation 5, E_c was the modulus of elasticity, u_c represented the Poisson's ratio, and h was the orthogonal distance between centroid of elements to the interface line.

$$\boldsymbol{\delta}_c = \sum_{i}^{2} \mathbf{B}_i \cdot \mathbf{u}_i \tag{1}$$

$$\mathbf{B}_1 = \begin{bmatrix} -l_1 & -m_1 & \{l_1(y-y_{1G}) - m_1(x-x_{1G})\} \\ -l_2 & -m_2 & \{l_2(y-y_{1G}) - m_2(x-x_{1G})\} \end{bmatrix} \quad \text{and} \tag{2}$$

$$\mathbf{B}_2 = \begin{bmatrix} l_1 & m_1 & \{-l_1(y-y_{2G}) + m_1(x-x_{2G})\} \\ l_2 & m_2 & \{-l_2(y-y_{2G}) + m_2(x-x_{2G})\} \end{bmatrix}$$

$$\boldsymbol{\varepsilon}_c = \frac{\boldsymbol{\delta}_c}{h} = \frac{\boldsymbol{\delta}_c}{(h_1 + h_2)} \tag{3}$$

$$\boldsymbol{\sigma}_c = \mathbf{D}_c \cdot \boldsymbol{\varepsilon}_c \tag{4}$$

$$\mathbf{D}_c = \begin{bmatrix} \left(\frac{E_c}{1-\nu_c^2}\right)\frac{1}{h} & 0 \\ 0 & \left(\frac{E_c}{1+\nu_c}\right)\frac{1}{h} \end{bmatrix} \tag{5}$$

Steel rebar in this study was modeled as an equivalent orthotropic plane stress element (Purnomo *et al.*, 2023a). Shear response in the element was transferred through dowel action where β_s expressed the dowel effect coefficient. In addition, recommended value of β_s was estimated using Equation 6, where d and a_m were the diameter of steel bar and approximated zone height (about 100 ~ 200 mm), respectively. Stress-strain matrix was expressed in Equation 7, where $\mathbf{D}_s$ represented the material matrix defined by Equation 8.

$$\beta_s = \frac{3}{4}\left(\frac{d}{a_m}\right)^2 \tag{6}$$

$$\boldsymbol{\sigma}_s = \mathbf{D}_s \cdot \boldsymbol{\varepsilon}_s \tag{7}$$

$$\mathbf{D}_s = E_s \cos^2\theta \begin{bmatrix} \cos^2\theta + \beta_s \sin^2\theta & (\beta_s - 1)\cos\theta\sin\theta \\ (\beta_s - 1)\cos\theta\sin\theta & \sin^2\theta + \beta_s \cos^2\theta \end{bmatrix} \tag{8}$$

During this study, the results were evaluated at the location of springs. Simple averaging method was proposed by lumping the results at springs to adjacent nodes at the element interface. Figure 4 showed the results of re-evaluation procedure at the nodes. In the Figure 4, the results in the springs represented the evenly distributed field at the interface between adjacent elements. These values were summed to the common nodes, N_1 and N_2.

Stress-strain relationship in tension was modeled as a linear function until ultimate followed by a softening linear curve. The initial stiffness of concrete in the compressive zone was accessed up to stress F_{c1}, estimated to be 50% of the ultimate cylindrical compressive strength. Subsequently, concrete stiffness was reduced until compressive stress achieved F_{c2}, defined as 95% of the characteristic cylindrical compressive strength. After reaching this magnitude, constant stress was assumed until achieving ultimate concrete compressive strain. Further, linear softening was presumed followed by a residual stress of 20% F_c.

Uniaxial stress-strain relationship of steel rebars under normal stress was assumed to be elastic-perfectly-plastic in compressive and tensile stress. After reaching the yield stress, the material experienced plastic deformation without significantly increasing stress. In the case of shear stress, the stress-strain relationship behaved linearly until yielding and was perfectly plastic later. The preceding uniaxial stress-strain curve described material behavior under simple load conditions. Moreover, individual stress-strain relationship led to a less accurate outcome in a more complex response due to combined stresses such as normal and shear stress. To address this, the modified Mohr-Coulomb criteria were adopted to justify the production condition of springs under combined normal and shear stress.

3. Results and Discussion

3.1. Multicriteria Sensitivity Analysis

Sensitivity analysis is a method frequently used in numerical modeling of structures to determine relative importance of each input parameter, potential interactions, and effects on model responses. The analysis is an important step in computational mechanics and earthquake engineering. In addition, sensitivity analysis had long-term applications in structural engineering, specifically in reinforced-concrete structures applications. Majority-based dynamic sensitivity analyses on the properties of the structure. (Cao *et al.*, 2023; Huang *et al.*, 2023; Bagheri *et al.*, 2021; Suwondo *et al.*, 2021) determined sensitivity analysis of the parameters based on geometric characteristics of buildings, composite and prefabricated concrete components. Consequently (Casafont *et al.*, 2024) included the test set-up and experimental result in sensitivity study to accommodate imperfections.

Soil and uncertainty of structural parameter based on sensitivity analysis incorporating seismic responses was studied by (Zhao *et al.*, 2023; Mekki *et al.*, 2022). This investigation used maximum structure displacement as the single parameter and as a function of material as well as soil characteristics. The study incorporated the seismic response to soil and interaction based on seismic peak acceleration. Following this discussion, the method helped studies to reduce the area of uncertainty and highly important variables and further assisted in quantifying uncertainties by accelerating the entire process of results.

In previous years, contingent on potentiality, application, and applied methodology, as well as possible diverse various classifications had been proposed. (Frey and Patil, 2002) classified sensitivity analysis method into three groups, namely mathematical, statistical, and graphical. Model parameter corrections using the uncertainty qualification (UQ) of numerical simulations were an alternative for model validation (Ren *et al.*, 2023). In this study, the deterministic mathematical method was adopted for sensitivity analysis. The mathematical method was a method to evaluate sensitivity of Quantity of Interest (QoI) to the variation of an input parameter that influenced the output of numerical simulations. In this method, QoIs were typically computed numerically using parametric values to represent the entire input range. Three QoIs (see Figure 5) were considered in this study as follows.

1. Peak load (P_u) of the envelope of loading-unloading experimental results according to (Purwanto *et al.*, 2023),
2. Energy enclosed by occurrence of peak load (E_u),
3. Toughness of structure (energy required per volume until the structure collapsed, T_g).

From the three QoIs mentioned, energy enclosed by occurrence of the peak load was found to show the best prediction.

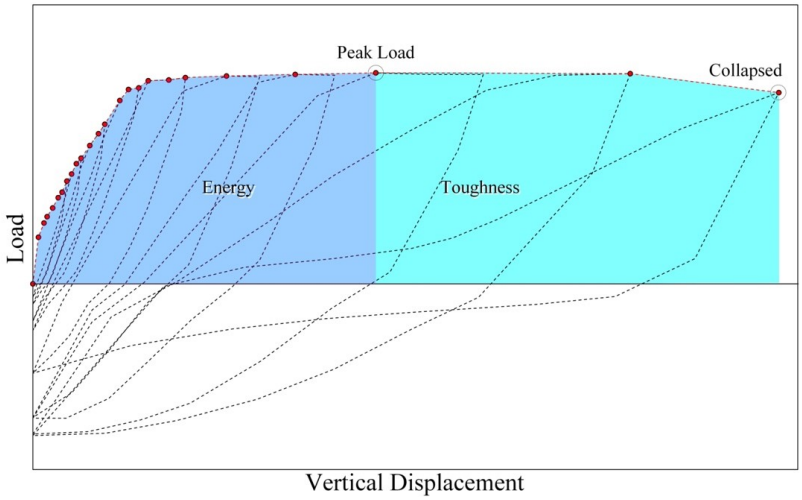

Figure 5 QoIs of strengthened beam-to-column model

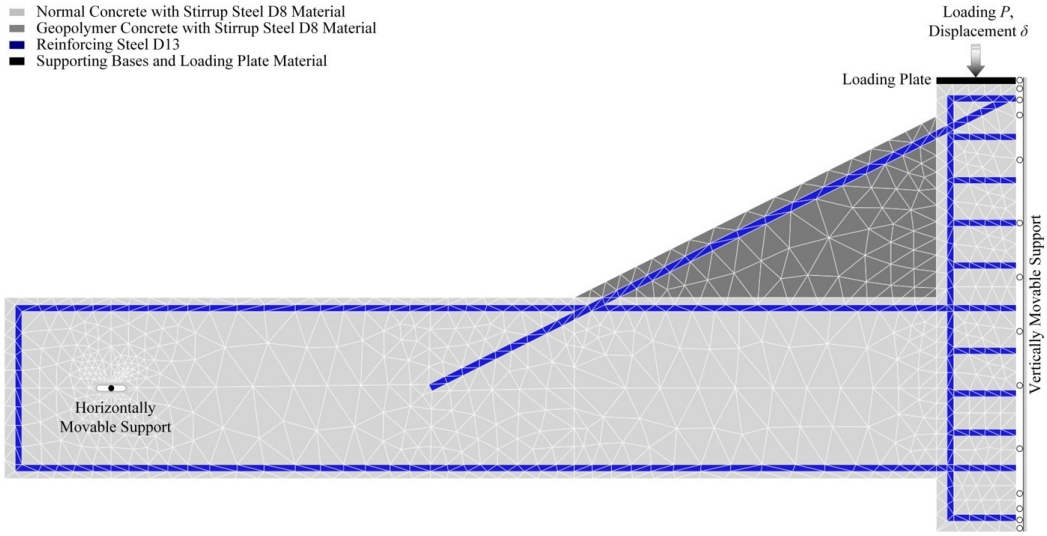

Figure 6 Symmetric haunch strengthened half-span beam-to-column RBSM

This study investigated sensitivity of input parameters by using a deterministic structural simulation applying the RBSM. During the process, RBSM was developed to represent haunch strengthened beam-to-column joint. Steel-reinforced geopolymer concrete haunch was constructed at both column sides under the beam. The beam-to-column joint was turned upside down for the convenience of a test loading setup in the laboratory that could only apply vertical loading downward. This downward load was applied to the upper column to simulate a negative bending moment at the beam members as in the real situation. Modeling only half of beam-to-column joint structure took advantage of symmetry of the problem. Figure 6 showed the haunch-strengthened beam-to-column model that was specifically designed for this study to represent the discretization scheme used by RBSM.

Tables 3, 4, and 5 showed mechanical properties of normal concrete, geopolymer concrete, and steel bar materials as the input parameters for running RBSM to conduct the sensitivity analysis and validate experimental results. The notations for the concrete in Table 3 and 4 are explained as follows.

- u_c = Poisson's ratio
- C = cohesive strength
- f = friction angle

- F_t = ultimate tensile strength
- c_1, c_2, c_3, c_4 = residual tensile stress coefficients
- e_{tu} = ultimate tensile strain
- E_{c1}, E_{c2} = 1st and 2nd compressive gradients
- F_{c1}, F_{c2} = 1st and 2nd yield stresses
- e_{cu} = ultimate yield strain

while the representations in Table 5 showed the properties of steel bars as

- E_s = modulus of elasticity of steel bars
- F_u = ultimate stress of steel bars
- β_s = dowel effect coefficient

Table 3 Mechanical properties of normal concrete

Properties [unit]	Calibrated Value	Reference	Note
u_c [-]	0.167	Trial Values (Yamamoto *et al.*, 2008)	
C [MPa]	1.54		
f [°]	37.0		
F_t [MPa]	2.072	Material Test (Purwanto *et al.*, 2023)	
c_1 [-]	1.07	Linear gradient line from F_t to 0 at e_{tu}	
c_2 [-]	Varies		
c_3 [-]	0.0		
c_4 [-]	0.0		
e_{tu} [-]	Varies		$20e_t$
E_{c1} [MPa]	24,559.0	Material Test (Purwanto *et al.*, 2023)	
E_{c2} [MPa]	12,279.5		with b = 0.5
F_{c1} [MPa]	Varies		(50% ~ 70%)F_c
F_{c2} [MPa]	31.11	Material Test (Purwanto *et al.*, 2023)	
e_{cu} [-]	0.0023262		

Table 4 Mechanical properties of geopolymer concrete

Properties [unit]	Calibrated Value	Reference	Note
u_c [-]	0.167	Trial Values (Yamamoto *et al.*, 2008)	
C [MPa]	2.51		
f [°]	42.0		
F_t [MPa]	2.380	Material Test (Purwanto *et al.*, 2023)	
c_1 [-]	1.07	Linear gradient line from F_t to 0 at e_{tu}	
c_2 [-]	Varies		
c_3 [-]	0.0		
c_4 [-]	0.0		
e_{tu} [-]	Varies		$20e_t$
E_{c1} [MPa]	25,091.0	Material Test (Purwanto *et al.*, 2023)	
E_{c2} [MPa]	12,545.5		with b = 0.5
F_{c1} [MPa]	Varies		(50% ~ 70%)F_c
F_{c2} [MPa]	31.11	Material Test (Purwanto *et al.*, 2023)	
e_{cu} [-]	0.0023252		

Before performing sensitivity analyses to input parameter shown in the aforementioned tables, several initial runs had been conducted to investigate the insensitive input parameters to the defined QoIs. Table 6 showed thirteen sensitive input parameters to QoIs for both normal and geopolymer concrete. Therefore, individual values were varied for sensitivity analyses during the study.

Table 5 Mechanical properties of steel reinforcing bars

Properties [unit]	Calibrated Value	Reference
E_s [MPa]	180,000	
F_u [MPa]	460.0	Material Test (Purwanto *et al.*, 2023)
β_s [-]	0.002	

Table 6 Sensitive mechanical properties of QoIs

Properties [unit]	Calibrated Value
F_t [MPa]	Varies
c_1 [-]	1.07
c_2 [-]	Varies
c_3 [-]	0.0
c_4 [-]	0.0
e_{tu} [-]	Varies
E_{c1} [MPa]	Varies
E_{c2} [MPa]	Varies
F_{c1} [MPa]	Varies
F_{c2} [MPa]	31.11 MPa (normal concrete), varies (geopolymer concrete)

Eighty-nine combinations of thirteen input parameters were extensively ran to generate the calibration data set. The results of QoIs (P_u, E_u, T_g) from RBSM were then normalized by experimental values obtained from the studies of (Purwanto *et al.*, 2023). Table 7 showed sensitivity analysis results where the most sensitive input parameters were varied in RBSM simulation.

Figure 7 showed the variances of the input parameters from the normalized QoI values, as the variances were sorted in descending order. The vertical red line signified the normalized value at 1.0, where simulation results of RBSM were close to experimental tests (Purwanto *et al.*, 2023).

Table 7 Results of sensitivity analyses

Properties [unit]	Normal Concrete	Geopolymer Concrete
F_t [MPa]	0.27 ~ 2.13	0.22 ~ 2.38
c_1 [-]	1.07	1.07
c_2 [-]	-10 ~ -500	-10 ~ -500
c_3 [-]	0.0	0.0
c_4 [-]	0.0	0.0
e_{tu} [-]	0.0121 ~ 0.1210	0.0143 ~ 0.1430
E_{c1} [MPa]	14,749 ~ 24,556	14,749 ~ 25,105
E_{c2} [MPa]	1,228 ~ 12,278	1,257 ~ 12,572
F_{c1} [MPa]	11.63 ~ 15.55	11.63 ~ 16.26
F_{c2} [MPa]	31.11	31.11 ~ 32.52

Figure 7 showed that the two most influencing and sensitive input parameters had the largest span of variance, including ultimate tensile stress F_t, and residual tensile stress coefficient c_2. Since QoIs of $\overline{P}_u$ and $\overline{E}_u$ originated from the same physical properties of model, c_2 had the most sensitivity to individual QoIs. However, toughness of the structure $\overline{T}_g$ was highly influenced by F_t. Tornado diagrams (Figure 8) were also constructed using the data applied in Figure 7. Moreover, the span of input parameters was centered on QoIs shown as vertical red lines.

Final, the ultimate tensile stress parameter was the most sensitive variable to QoIs using RBSM. The present results could help studies as a guide on how to simulate experimental model by applying RBSM.

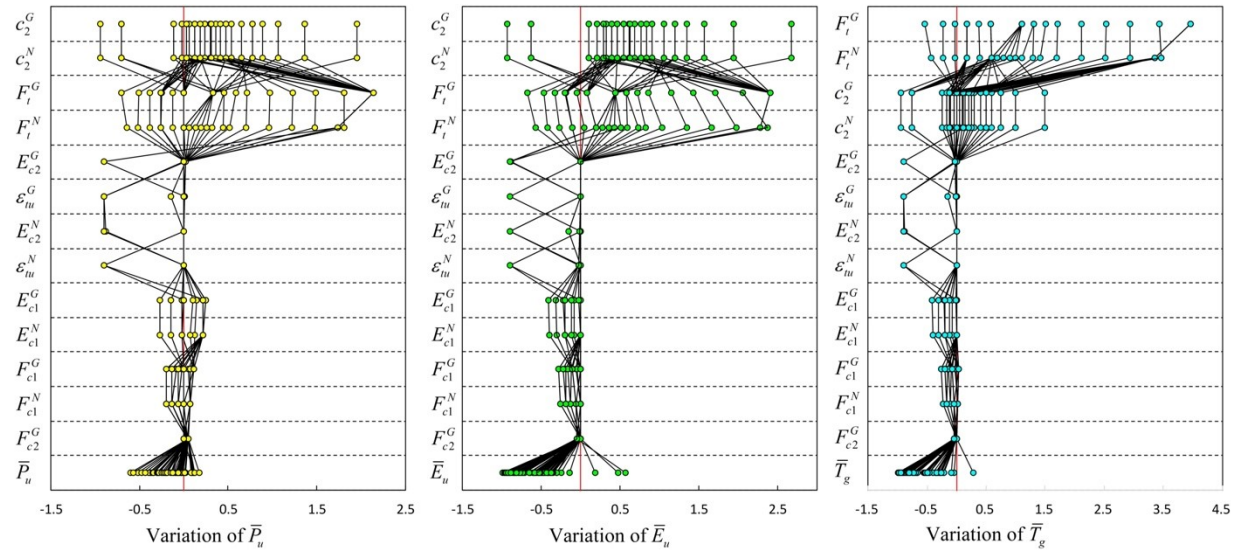

Figure 7 Results of QoIs from RBSM by running eighty-nine test cases

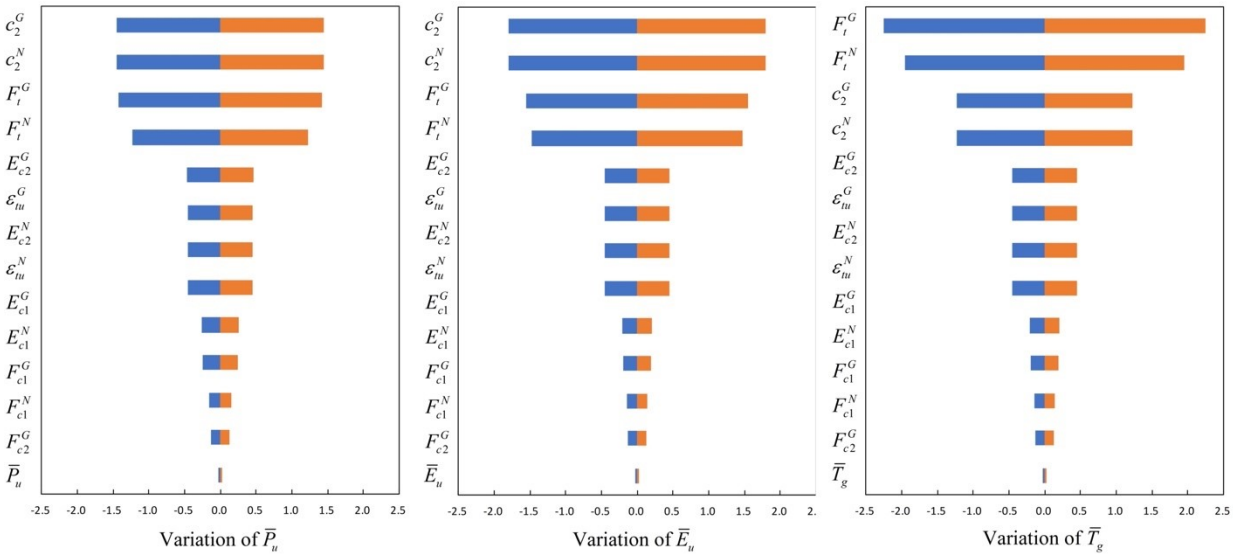

Figure 8 Tornado diagrams of QoIs from RBSM by running eighty-nine test cases

3.2. Validation to RBSM

Sensitivity analysis is a method frequently used in statistical-based studies, where the random data are usually generated to give QoI defined. Additionally, reliability analysis typically followed sensitivity analysis to develop a statistical model that could predict new occurrences without being analyzed using conventional methods.

During this study, sensitivity analysis results were used to validate QoIs of experimental investigations conducted by (Purwanto *et al.*, 2023). To validate experimental results of geopolymer concrete, haunch was developed to strengthen the connection between beam and column of a building structure. The output of the load-displacement of experimental works was then validated using RBSM simulations.

Table 8 showed the values of interpolated input parameters in which the values of QoIs were equal to 1.0s. In addition, the validation of experimental results could be conducted at three different conditions of QoIs with these interpolated sets of input parameters.

Table 8 Results of sensitivity analyses at QoIs were equal to 1.0 s

Properties [unit]	Normal Concrete			Geopolymer Concrete		
	$\overline{P}_u$ = 1.0	$\overline{E}_u$ = 1.0	$\overline{T}_g$ = 1.0	$\overline{P}_u$ = 1.0	$\overline{E}_u$ = 1.0	$\overline{T}_g$ = 1.0
F_t [MPa]	0.758	0.631	0.477	0.758	0.697	0.480
c_1 [-]	1.07	1.07	1.07	1.07	1.07	1.07
c_2 [-]	-169.5	-136.1	-200.0	-169.5	-136.1	-200.0
c_3 [-]	0.0	0.0	0.0	0.0	0.0	0.0
c_4 [-]	0.0	0.0	0.0	0.0	0.0	0.0
e_{tu} [-]	0.121	0.121	0.121	0.141	0.143	0.143
E_{c1} [MPa]	20,181	24,556	20,181	20,181	25,105	25,033
E_{c2} [MPa]	12,278	12,278	12,278	12,278	12,572	12,534
F_{c1} [MPa]	14.57	15.56	14.57	15.17	16.26	15.78
F_{c2} [MPa]	31.11	31.11	31.11	31.11	32.52	32.52

Numerical simulations in RBSM were run to signify predicted results close to experimental work results by using three sets of input parameters, which were shown in Table 8. The corresponding tensile stress-strain relationships which produced each QoI were equal to 1.0 during validation were shown in Figure 9. Meanwhile, Figure 10 showed envelope of loading-unloading scheme was close to the results when $\overline{E}_u$ = 1.0, which was represented by vertical red lines.

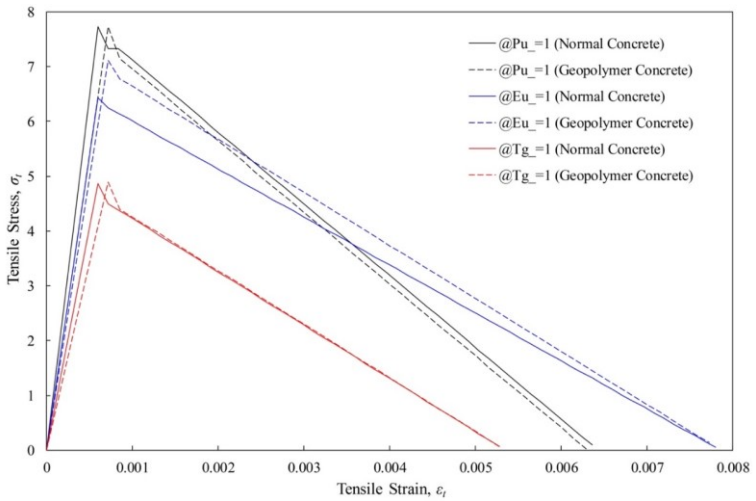

Figure 9 Tensile stress-strain relationships of concrete material validated for RBSM

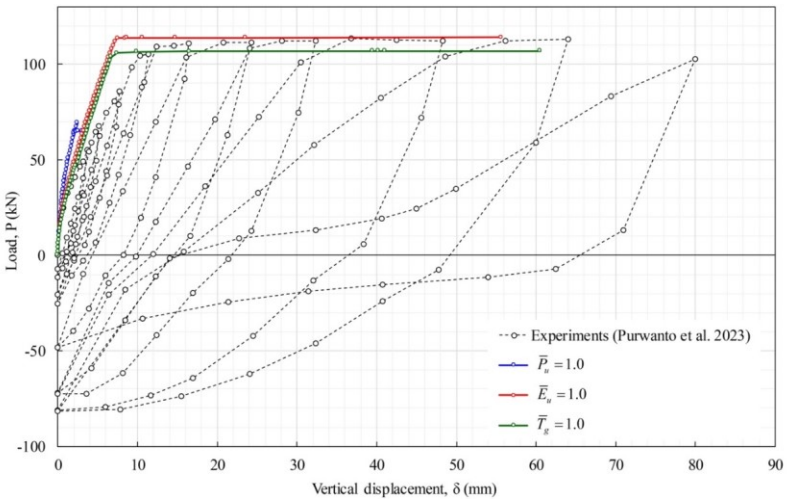

Figure 10 Comparison between envelope curves of experimental results and RBSM

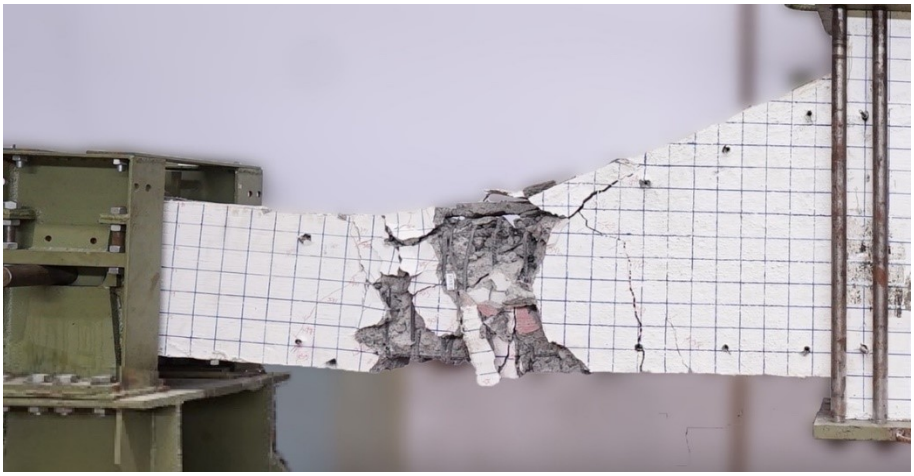

(a) Failure pattern of haunch-strengthened beam-to-column joint.

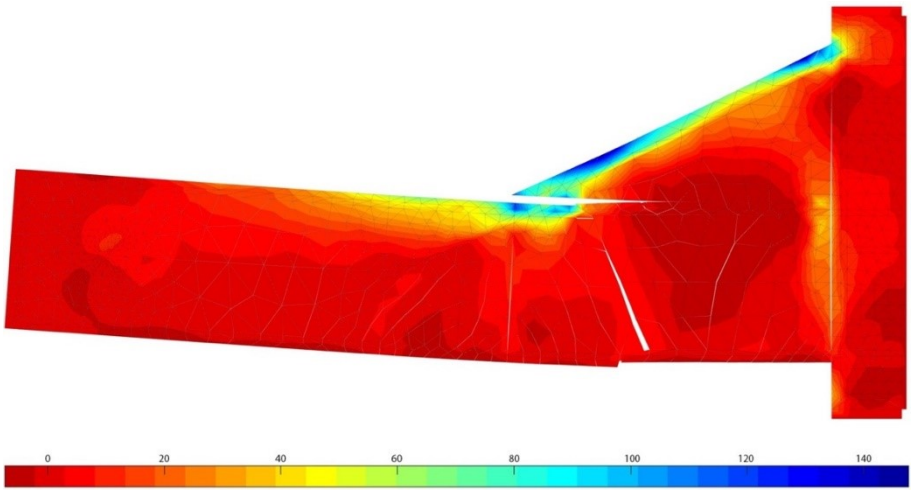

(b) Normal stresses of concrete in RBSM at $\overline{E}_u$ = 1.0 condition.

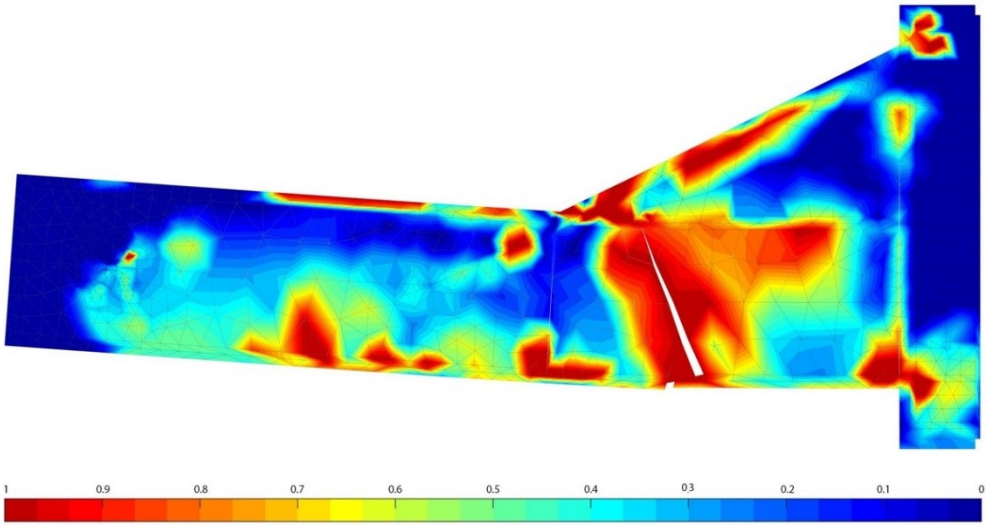

(c) Concrete plasticity index of RBSM at $\overline{E}_u$ = 1.0 condition.

Figure 11 Comparisons of failure patterns and plasticity conditions between test and validation results of haunch-strengthened beam-to-column joint

Figure 10 showed the results of sensitivity analysis when $\overline{E}_u$ = 1.0 was selected to validate experimental results (Purwanto *et al.*, 2023). In addition, Figure 11 signified the

representative failure patterns of test and validation results by using RBSM. As identified in Figure 11a, test specimen showed the compressive and tensile failure of beam, which occurred apart from joint with the column. The test also signified that by haunch strengthening beam-to-column, failure location moved farther from column where maximum negative bending moment occurred. Following this discussion, re-location of failure location had already shown that haunch could increase beam-to-column joint capacity.

In Figure 11b, the results of RBSM showed normal stress distribution in concrete matrix where at the end of the haunch, the stress concentration in compression could be observed. This process caused spalling of concrete cover, some cracking patterns were also shown at the bottom of beam that was subjected to tension due to the bending moment. Figure 11c showed concrete plasticity index of RBSM where concrete failures were spreading, which also signified the effectiveness of the proposed haunch strengthening method.

4. Conclusions

In conclusion, multicriteria sensitivity analyses were proven efficient in quantifying the importance of input parameter, potential interaction and effects on the behavior of load-displacement response of structure. The information on this unsureness of variables could be used in improving continuing experimental and minimizing uncertainty of the mentioned parameters. Moreover, sensitivity evaluation of Qols efficiently obtained the best value for each of the three sets of input parameters including peak load of the backbone from the loading-unloading envelope $\overline{P}_u$, energy dissipation before ultimate load $\overline{E}_u$, and toughness until the collapse of member $\overline{T}_g$. The method was shown through analysis of a geopolymer beam-to-column load-displacement response of a haunch connection. Following this discussion, multicriteria method effectively handled complex composite structural elements and captured the variations in concrete strength, including the use of both conventional as well as geopolymer concrete with high accuracy. The application signified the usefulness in constructing accurate behavior of composite concrete member with high precision, incorporating the imperfections of actual laboratory-based load-displacement relationship. Relating to this discussion, the proposed method could be generalized and implemented into any FEA software or subroutines of nonlinear simulation programs.

Acknowledgements

The authors are grateful to the following institutions for individual financial support, including Institute for Study and Community Service (LPPM), Universitas Diponegoro with the scheme of Riset Publikasi Internasional Bereputasi Tinggi (RPIBT) through the decreed number 609-125/UN7.D2/PP/VII/2024.

Conflict of Interest

The authors declared no conflicts of interest.

References

Ahmed, Z., Madkour, H., Farah, K., Othman, A., 2020. Numerical Analysis of RC Beams Reinforced with CFRP Rods. *International Research Journal of Engineering and*

Technology, Volume 07(1), pp. 1373–1377. https://www.irjet.net/archives/V7/i1/IRJET-V7I1236.pdf

Aziz, M.W., Suprobo, P., Tajunnisa, Y., 2022. Numerical Analysis Study of the Effect Geopolymer Concrete Compressive Strength on Ductility of Reinforced Concrete Beams. *Journal of Civil Engineering*, Volume 37(1), pp. 33-38. https://doi.org/10.12962/j20861206.v37i1.12193

Bagheri, A., Genikomsakis, K.N., Feldheim, V., Loakimidis, C.S., 2021. Sensitivity Analysis of 4R3C Model Parameters with Respect to Structure and Geometric Characteristics of Buildings. *Energies*, Volume 14(3), p. 657. https://doi.org/10.3390/en14030657

Blagojević, P., Blagojević, N., Kukaras, D., 2021. Flexural Behavior of Steel Fiber Reinforced Concrete Beams: Probabilistic Numerical Modeling And Sensitivity Analysis. *Applied Sciences*, Volume 11(20), p. 9591. https://doi.org/10.3390/app11209591

Cao, X.X., Yang, D.H., Wu, C.F., Yang, K. 2023. Sensitivity Analysis of Design Parameters of Prefabricated Cantilever Structure. *In***:** Journal of Physics: Conference Series, Volume 2476, p. 012043. https://doi.org/10.1088/1742-6596/2476/1/012043

Casafont, M., Marimon, F., Bové, O., Ferrer, M., Centelles, X., 2024. Local Buckling of Cold-Formed Steel Trapezoidal Sheets: Data for Finite Element Model Validation. *Data in Brief*, Volume 53, p. 110075. https://doi.org/10.1016/j.dib.2024.110075

Chong, K., Suryanto, B., Tambusay, A., Suprobo, P., 2022. Nonlinear Analysis of Reinforced Geopolymer Concrete Beams. *Civil Engineering Dimension*, Volume 24(1), pp. 1–10. https://doi.org/10.9744/ced.24.1.1-10

Darmawan, M.S., Tajunnisa, Y., Suprobo, P., Sutrisno, W., Aziz, M.W., 2022. Comparative Study of Flexural Performance of Geopolymer And Portland Cement Concrete Beam Using Finite Element Analysis. *International Journal of GEOMATE*, Volume 23(95), pp. 1–9. https://doi.org/10.21660/2022.95.j2340

Farah, K., Sato, Y., 2007. Numerical Simulation of Debonding Failure of Reinforced Concrete Beams Strengthened with Externally Bonded FRP. *In:* Proceedings of the 1st Asia-Pacific Conference on FRP in Structures, APFIS 2007. https://api.semanticscholar.org/CorpusID:14136253

Feng, D.-C., Fu, B., 2020. Shear Strength of Internal Reinforced Concrete Beam-Column Joints: Intelligent Modeling Approach and Sensitivity Analysis. *Advances in Civil Engineering*, Volume 2020(1), p. 8850417. https://doi.org/10.1155/2020/8850417

Ferro, R.M., Pavanello, R., 2023. A Simple and Efficient Structural Topology Optimization Implementation Using Open-Source Software for all Steps of the Algorithm: Modeling, Sensitivity Analysis and Optimization. *Computer Modeling in Engineering & Sciences*, Volume 136(2), pp. 1371–1397. https://doi.org/10.32604/cmes.2023.026043

Frey, H.C., Patil, S.R., 2002. Identification and Review of Sensitivity Analysis Methods. *Risk Analysis*, Volume 22(3), pp. 553–578. https://doi.org/https://doi.org/10.1111/0272-4332.00039

Fu, L., Yin, Q., Zheng, J., Wang, D., Wang, H., 2023. Applicability of 3D RBSM on Evaluation of Size Effect for RC Deep Beam Loaded in Shear. *Yingyong Lixue Xuebao/Chinese Journal of Applied Mechanics*, Volume 40(4). pp. 947–955. https://chinaxiv.org/abs/202311.00077?locale=en

Ghafoor, M.T., Fujiyama, C., 2023. Mix Design Process for Sustainable Self-Compacting Geopolymer Concrete. *Heliyon*, Volume 9(11), p. e22206. https://doi.org/10.1016/j.heliyon.2023.e22206

Gong, F., Wang, Y., Zhang, D., Ueda, T., 2015. Mesoscale Simulation of Deformation for Mortar and Concrete Under Cyclic Freezing and Thawing Stress. *Journal of Advanced Concrete Technology*, Volume 13(6), pp. 291–304. https://doi.org/10.3151/jact.13.291

Hassan, A., Arif, M., Shariq, M., Alomayri, T., 2022. Experimental Test and Finite Element Modelling Prediction on Geopolymer Concrete Beams Subject to Flexural Loading. *Innovative Infrastructure Solutions*, Volume 7(1), p. 13. https://doi.org/10.1007/s41062-021-00615-9

Huang, M., Yao, G., Gao, K., Wang, M., 2023. An Adaptive Subinterval Finite Element Method Based on Dynamic Sensitivity Analysis for Structures with Uncertain-But-Bounded Parameters. *Applied Sciences*, Volume 13(13), p. 7426. https://doi.org/10.3390/app13137426

Jaiswal, D.K., Murty, C.V.R., 2024. Refinement in the Understanding of Confinement of Concrete. *Structures*, Volume 62, p. 106115. https://doi.org/10.1016/j.istruc.2024.106115

Jiang, C., Avadh, K., Nagai, K., 2023. A Mesoscale Simulation of the FRP-To-Concrete Interfacial Debonding Propagation Process by 3D RBSM. *Composite Structures*, Volume 304(Part 2), p. 116336. https://doi.org/10.1016/j.compstruct.2022.116336

Kagermanov, A., Markovic, I., 2023. An Overview on Finite Element-Modelling Techniques for Structural Capacity Assessment of Corroded Reinforced Concrete Structures. *Structure and Infrastructure Engineering*, Volume 19(11), pp. 1585-1599. https://doi.org/10.1080/15732479.2022.2045612

Kanagaraj, B., Anand, N., Alengaram, U.J., Samuvel Raj, R., Jayakumar, G., 2023. Promulgation of Engineering and Sustainable Performances of Self-Compacting Geopolymer Concrete. *Journal of Building Engineering*, Volume 68, p. 106093. https://doi.org/10.1016/j.jobe.2023.106093

Kumar, A.A., Raguraam, S., 2018. Comparison of Fresh and Hardened Properties of Normal, Self Compacting and Smart Dynamic Concrete. *International Journal of Technology*, Volume 9(4), pp. 707–714. https://doi.org/10.14716/ijtech.v9i4.566

Li, K., Long, Y., Wang, H., Wang, Y., 2021. Modeling and Sensitivity Analysis of Concrete Creep with Machine Learning Methods. *Journal of Materials in Civil Engineering*, Volume 33(8). https://doi.org/10.1061/(asce)mt.1943-5533.0003843

Mekki, M., Zoutat, M., Elachachi, S.M., Hemsas, M., 2022. Sensitivity Analysis of Uncertain Material RC Structure and Soil Parameters on Seismic Response of Soil-Structure Interaction Systems. *Periodica Polytechnica Civil Engineering*, Volume 66(3), pp. 739–751. https://doi.org/10.3311/PPci.20113

Nafees, A., Amin, M.N., Khan, K., Nazir, K., Ali, M., Javed, M.F., Aslam, F., Musarat, M.A., Vatin, N.I., 2022. Modeling of mechanical properties of silica fume-based green concrete using machine learning techniques. *Polymers*, Volume 14(1), p. 30. https://doi.org/10.3390/polym14010030

Ottosen, N.S., Ristinmaa, M., 2005. *The Mechanics of Constitutive Modeling, The Mechanics Of Constitutive Modeling*. Elsevier Science, Amsterdam, The Netherlands. https://doi.org/10.1016/B978-0-08-044606-6.X5000-0

Petrus, H.T.B.M., Olvianas, M., Astuti, W., Nurpratama, M.I., 2021. Valorization of Geothermal Silica and Natural Bentonite Through Geopolymerization: A Characterization Study and Response Surface Design. *International Journal of Technology*, Volume 12(1), pp. 195–206. https://doi.org/10.14716/ijtech.v12i1.3537

Purnomo, J., Han, A., Yamakawa, R., Gan, B.S., 2023a. Systematic Calibration Procedure for CFRP Sheets and Rods Strengthened RC T-Beams by using RBSM. *Mechanics of Advanced Materials and Structures*, Volume 30(9), pp. 1913–1929. https://doi.org/10.1080/15376494.2022.2111483

Purnomo, J., Han, A., Gan, B.S., Hardjito, D., 2023b. The Effects of Various Parameters in Sensitivity Analysis of Plain Concrete Beam Using Rigid Body Spring Model. *In:* IOP

Conference Series: Earth and Environmental Science, Volume 1195, p. 012016. https://doi.org/10.1088/1755-1315/1195/1/012016

Purwanto, 2021. *Beam-Column External Reinforcement Using A Self-Compacting Geopolymer Concrete Haunch*. Doctorate Thesis. Doctorate Thesis, Civil Engineering, Diponegoro University, Indonesia

Purwanto, Ekaputri, J.J., Nuroji, Indriyantho, B.R., Han, A.L., Gan, B.S., 2022. Shear-Bond Behavior of Self-Compacting Geopolymer Concrete to Conventional Concrete. *Construction and Building Materials*, Volume 321, p. 126167. https://doi.org/10.1016/j.conbuildmat.2021.126167

Purwanto, Indarto, H., 2019. Study of Proportional Variation of Geopolymer Concrete Which Self Compacting Concrete. *Journal of Advanced Civil and Environmental Engineering*, Volume 2(2), pp. 65-75. https://doi.org/10.30659/jacee.2.2.65-75

Purwanto, P., Ekaputri, J.J., Nuroji, N., Indriyantho, B.R., Gan, B.S., Han, A.L., 2023. Geopolymer Haunch Beam–Column Connection Behavior. *Arabian Journal for Science and Engineering*, Volume 48, pp. 13633–13648. https://doi.org/10.1007/s13369-023-07921-7

Ren, C., Xiong, F., Wang, Y., Li, N., Jiang, B., Guo, Z., 2023. Model Validation Method by Considering Uncertainty for Numerical Simulation. *Xibei Gongye Daxue Xuebao/Journal of Northwestern Polytechnical University*, Volume 41(5), pp. 987–995. https://doi.org/10.1051/jnwpu/20234150987

Sarraz, A., Nakamura, H., Kanakubo, T., Miura, T., Kobayashi, H., 2022. Bond Behavior Simulation of Deformed Rebar in Fiber-Reinforced Cementitious Composites Using Three-Dimensional Meso-Scale Model. *Cement and Concrete Composites*, Volume 131, p. 104589. https://doi.org/10.1016/j.cemconcomp.2022.104589

Sarraz, A., Nakamura, H., Miura, T., 2023. Mesoscale Modelling of SFRC Based on 3D RBSM Considering the Effects of Fiber Shape and Orientation. *Cement and Concrete Composites*, Volume 139, p. 105039. https://doi.org/10.1016/j.cemconcomp.2023.105039

Suwondo, R., Cunningham, L., Gillie, M., Suangga, M., Hidayat, I., 2021. Model Parameter Sensitivity for Structural Analysis of Composite Slab Structures in Fire. *International Journal of Technology*, Volume 12(2), pp. 339–348. https://doi.org/10.14716/ijtech.v12i2.3919

Takeuchi, N., 2005. Discretized Limit Analysis Method for Reinforced Concrete Structures*. Computational Mechanic Lecture Series 7.* Maruzen, Tokyo

Thakur, M., Bawa, S., 2022. Self-compacting Geopolymer Concrete: A review. *In:* Materials Today: Proceedings, Volume 59(Part 3), pp. 1683–1693. https://doi.org/10.1016/j.matpr.2022.03.400

Thang, N.H., Thach, B.K., Minh, D.Q., 2021. Influence of Curing Regimes on Engineering and Microstructural Properties of Geopolymer-Based Materials from Water Treatment Residue and Fly Ash. *International Journal of Technology*, Volume 12(4), pp. 700–710. https://doi.org/10.14716/ijtech.v12i4.4626

Ulhaq, N.D., Andayani, R., 2021. Normal Concrete Mix Design Based on the Isoresponse of Slump as a Function of Specific Surface Area of Aggregate and Cement Paste-Aggregate Ratio. *International Journal of Technology*, Volume 12(3), pp. 495–505. https://doi.org/10.14716/ijtech.v12i3.3355

Venkatachalam, S., Vishnuvardhan, K., Amarapathi, G.D., Mahesh, S.R., Deepasari, M., 2021. Experimental and Finite Element Modelling of Reinforced Geopolymer Concrete Beam. Materials Today: Proceedings, Volume 45(Part 7), pp. 6500–6506. https://doi.org/10.1016/j.matpr.2020.11.449

Yamamoto, Y., Nakamura, H., Kuroda, I., Furuya, N., 2008. Analysis of Compression Failure of Concrete by Three-dimensional Rigid Body Spring Model. *Doboku Gakkai Ronbunshuu E*, Volume 64(4), pp. 612–630. https://doi.org/10.2208/jsceje.64.612

Wei, X., Ren, X., 2023. Confinement Enhanced Damage-Plasticity Model for Concrete. Mechanics of Materials, Volume 179, p. 104589. https://doi.org/10.1016/j.mechmat.2023.104589

Zhao, J., Cui, C., Zhang, P., Wang, K., Zhao, M., 2023. Parameter Sensitivity Analysis of the Seismic Response of a Piled Wharf Structure. *Buildings*, Volume 13(2), p. 349. https://doi.org/10.3390/buildings13020349

Zheng, J., Fu, L., Wang, D., 2021. The Application of Rigid-Body-Spring-Method on the Shear Failure Size Effect of RC Cantilever Beams. *Yingyong Lixue Xuebao/Chinese Journal of Applied Mechanics*, Volume 38(2), pp. 515–522. https://doi.org/10.11776/cjam.38.02.B174